This document is the accepted manuscript version of the following article:
Weber, U. W., Cook, P. G., Brennwald, M. S., Kipfer, R., & Stieglitz, T. C. (2019). A novel approach to quantify air-water gas exchange in shallow surface waters using high-resolution time series of dissolved atmospheric gases. Environmental Science and Technology, 53(3), 1463-1470. https://doi.org/10.1021/acs.est.8b05318

A Novel Approach to Quantify Air-Water Gas Exchange in Shallow Surface Waters Using High-Resolution Time Series of Dissolved Atmospheric Gases

Ulrich W. Weber,[*,‡] Peter G. Cook,[¶,§] Matthias S. Brennwald,[‡] Rolf Kipfer,[‡,∥] and Thomas C. Stieglitz[⊥,#]

‡*Department of Water Resources and Drinking Water, Eawag, Swiss Federal Institute of Aquatic Science and Technology, Dübendorf 8600, Switzerland*

¶*National Centre for Groundwater Research and Training (NCGRT), School of the Environment, Flinders University, Adelaide SA 5001, Australia*

§*Aix-Marseille Université, IMéRA, Marseille 13004, France*

∥*Institute for Geochemistry and Petrology, ETH Zurich, Zurich 8092, Switzerland*

⊥*Centre Européen de Recherche et d'Enseignement des Géosciences de l'Environnement (CEREGE), CNRS, IRD, INRA, Coll France, Aix en Provence 13545, France*

#*Centre for Tropical Water and Aquatic Ecosystem Research, James Cook University, Townsville QLD 4811, Australia*

E-mail: uli.weber@eawag.ch

Phone: +49 (0) 176 99123345

Abstract

Gas exchange across the air-water interface is a key process determining the release of greenhouse gases from surface waters, and a fundamental component of gas dynamics

in aquatic systems. In order to experimentally quantify the gas transfer velocity in a wide range of aquatic settings, a novel method is presented based on recently developed techniques for the *in situ*, near-continuous measurement of dissolved (noble) gases with a field-portable mass spectrometer.

Variations in observed dissolved gas concentrations are damped and lagged with respect to equilibrium concentrations, being the result of (a) temperature (and thus solubility) variations, (b) water depth and (c) the specific gas transfer velocity (k_i). The method fits a model to the measured gas concentrations to derive the gas transfer velocity from the amplitude and the phase lag between observed and equilibrium concentrations. With the current experimental setup, the method is sensitive to gas transfer velocities of $0.05 - 9\,m/d$ (for N_2), at a water depth of $1\,m$, and a given daily water temperature variation of $10\,°C$. Experiments were carried out (a) in a controlled experiment to prove the concept and to confirm the capability to determine low transfer velocities and (b) in a field study in a shallow coastal lagoon covering a range of transfer velocities, demonstrating the field applicability of the method.

Introduction

Gas exchange across the air-water interface is a key process coupling atmospheric and aquatic gas cycles. Accurate knowledge of gas exchange rates is required to determine mass balances of dissolved gases in aquatic systems, which can in turn be used to estimate fluxes between groundwater reservoirs and surface water.[1–3] Surface water bodies can be sources or sinks for gases:[4,5] whereas release of methane and carbon dioxide from water bodies is an important source of greenhouse gases to the atmosphere, the reverse flux of oxygen and nitrogen from atmosphere to water is an important factor in water quality and ecosystem functioning.[6]

The gas transfer velocity for open ocean conditions is well parametrized in its dependence on wind speed.[7] Furthermore, numerous empirical relationships are available for rivers where gas exchange is primarily a function of turbulent mixing due to water flow.[8] In contrast, for

shallow open water surfaces like shallow lakes and, importantly, the coastal zone of oceans, a parametrization is currently not available that fully takes into account the physical processes driving gas exchange, which differ significantly from those in the open ocean or rivers. In these systems, the influence of other environmental parameters, e.g. rain,[9,10] current velocity or bottom roughness, on near surface turbulence increases due to the decreased wind fetch and lower water depth,[11] and this fundamentally impacts air/water partitioning.

A commonly used method for estimating the transfer velocity at specific sites over short time scales consists of injecting and monitoring trace gases.[11–14] Besides being experimentally demanding[11] and sometimes being subject to environmental regulation (e.g. SF_6), trace gas injection may contaminate the sites and render future experiments impossible.[15]

Recently, in studies primarily targeting the estimation of residence times of water within catchments, it was noted that diurnal variations in water temperature in rivers produced periodically varying concentrations of dissolved gases, which were damped and lagged in comparison with atmospheric equilibrium concentrations.[15]

Variations of the gas concentrations are a function of the temperature variation, the temperature-dependence of gas solubility in water, and the gas transfer velocity. In principle, synchronous measurement of time series of temperature and concentrations of dissolved gases therefore allows the gas transfer velocity to be estimated. Recent advances in determining gas concentrations have led to the development of field portable MIMS (membrane inlet mass spectrometry) systems that can measure concentrations of He, Ar, Kr, N_2, O_2, CO_2 and CH_4 with relatively high accuracy and precision.[16–18] These novel techniques allow in-situ, real-time measurement of gas concentration time series with a temporal resolution of a few minutes and make subsequent laboratory analysis redundant.

The objective of this study is to combine the approach to calculate gas exchange rates[15] with those novel measurement techniques. Further, we aim to establish the environmental conditions for which gas transfer velocities can be derived using the diurnal gas dynamics (DGD). We first calculate the sensitivity and resolution of the presented method in a theo-

retical setting. The performance and the experimental requirements are then demonstrated in a controlled experiment and in the large, shallow La Palme lagoon at the Mediterranean Sea in southern France.

Theory

The gas flux of species i between air and water is caused by a disequilibrium of aquatic and atmospheric gas concentrations:[19]

$$F_i = k_i \cdot \Delta C_i = k_i \cdot (C_{w,i} - C_{eq,i}), \tag{1}$$

with F_i being the gas flux, $C_{w,i}$ the concentration in the water, and $C_{eq,i}$ the concentration in air saturated water, and k_i is the gas transfer velocity, which reflects the rate of exchange. This basic relation, even though not accounting for bubble-mediated gas fluxes, is used to determine fluxes at regional-to-global scales.[7]

If the water is well mixed, the flux can also be written as

$$F_i = \frac{dC_{w,i}}{dt} \cdot h, \tag{2}$$

with h being the water depth of the exchanging water mass ('mixed layer'). Equating 1 and 2 yields

$$\frac{dC_{w,i}}{dt} = \frac{k_i}{h} \cdot (C_{w,i} - C_{eq,i}). \tag{3}$$

The equilibrium gas concentrations depend on the temperature (T_w) and the salinity (S) of the water and the partial pressure of each gas, and are determined by Henry's law,[20]

$$C_{eq,i} = \frac{p_i}{H_i(T_w, S)}. \tag{4}$$

The Henry's coefficient (H_i) is specific to each gas species.[21–23] p_i is the partial pressure of

species i in the atmosphere and is given by $p_i = (p_{atm} - e_s(T_w))v_i$, with p_{atm} the local total atmospheric pressure, $e_s(T_w)$ the water vapor pressure, and v_i the volume fraction of gas i in dry air.[20]

Diurnal variation in $C_{eq,i}$ for the different gases is largely a function of the temperature dependence of their solubilities.[20] The magnitude of the diurnal variation in $C_{eq,i}$ for the noble gases will therefore be greatest for Xe and Kr, less for Ar and least for He and Ne. The temperature dependence of the solubility of N_2 is similar to that of Ar.

To convert the transfer velocity derived from one gas species to another commonly the respective Schmidt numbers are used. The Schmidt number is defined as the ratio of kinematic viscosity of water, divided by the diffusion coefficient of the gas in water. The transfer velocities ($k_{1,2}$) of gas 1 and 2 are linked to each other via their Schmidt numbers ($Sc_{1,2}$) in a power law dependence with the Schmidt number exponent (n):

$$\frac{k_1}{k_2} = \left(\frac{Sc_1}{Sc_2}\right)^{-n} \tag{5}$$

where n theoretically ranges from $1/2 < n < 2/3$.[24] However, n decreases rapidly to 1/2 with the onset of waves[24] (free surface condition). The ratio of (Sc_1/Sc_2) is approximately constant with temperature.[25]

While concentration gradients for reactive gases can also occur due to biogeochemical reactions, i.e. photosynthetic production in the case of O_2 and production by denitrification in the case of N_2, the concentrations of the (atmospheric) noble gases are only controlled by physical processes, specifically radioactive decay and air-water gas-exchange.

Method

Modeling

An ordinary differential equation solver is used to derive the results for the expected in-situ concentrations ($C_{w,i}$) by solving Eq. 3. The mean of the first ten measured $C_{w,i}$ of a time series is used as the initial gas concentration.

The parameters for the equilibrium concentrations ($C_{eq,i}$) (cf. Eq. 4) and the water depth are given by the local environmental system, so that the transfer velocity (k_i) and $C_{w,i}$ remain as the only free parameters.

The model is fit to the measured concentrations by varying k_i. The fit is optimized by minimizing the sum of squared errors (SSE) between the measured and modeled concentrations of the respective gas species.

The uncertainty of the best-fit gas exchange rate k_i^* (95 % confidence interval) was determined from the scatter of the observed concentrations relative to the best-fit model curves.[26] The measured gas concentrations time series of the field study were filtered with a Savitzky-Golay filter (order 3, frame length 21) to reduce noise.[27]

Experimental Method

The concentrations of dissolved N_2, ^{40}Ar and ^{84}Kr in the water were analyzed with a portable 'miniRUEDI' mass spectrometer[16] (Gasometrix GmbH) using the gas-equilibrium membrane-inlet mass spectrometry method (GE-MIMS).[16,28,29] For later calculations ^{40}Ar and ^{84}Kr are converted to elemental concentration.[20]

During the experiments a submersible pump was used to continuously sample the water through a membrane contactor module (Liqui-Cel G542), in which the gases equilibrate between the water and a small gas headspace according to Henry's law. The partial pressures of N_2, ^{40}Ar and ^{84}Kr in the headspace were quantified from the mass spectrometer readings by peak-height comparison relative to analyses of ambient air, which was used as calibration

standard.[16] The analytical sequence was a continuously repeating cycle consisting of one air-standard analysis block, followed by three water sample analysis blocks, followed by one ambient air sample analysis block to assess the analytical performance.[16] Each of these analysis blocks were $8\,min$ long.

The partial pressures observed in the headspaces of the membrane modules were converted to dissolved gas concentrations using the gas-specific Henry's law coefficients at the temperature of the water in the membrane modules. The partial pressures obtained from the ambient-air samples were used to estimate the analytical uncertainties of the dissolved-gas concentrations as $1\,\%$ for N_2, $2.5\,\%$ for Ar and $4\,\%$ for Kr.

In the controlled experiment and the field study at La Palme lagoon, in-situ water temperature, salinity and atmospheric pressure were recorded by sensors every $10\,min$ in order to calculate $C_{eq,i}$ using Eq. 4.

Controlled Experiment

A concept test of the DGD method to determine gas transfer velocities was conducted outside the Swiss Federal Institute of Aquatic Science and Technology (Eawag) in Dübendorf, Switzerland. For that purpose, a small tank ($height = 15\,cm$, $length = 60\,cm$, $width = 40\,cm$) with a black shell was used. The small volume ($0.036\,m^3$) and the black color of the tank caused a large temperature increase of the water in response to sun irradiation and a rapid decline in water temperature as air temperature dropped at night.

The water in the tub was circulated through the membrane module, where the gases equilibrate for measurement. Cavitation was not observed with a pumping rate of about $2\,l/min$. The forced circulation caused an increase in turbulence in the water, producing a well mixed water body. This turbulence is assumed to be constant over time, as the pumping rate was kept constant. The development of (breaking) waves was heavily suppressed by the walls and the small surface area of the tank.

Field Study at La Palme Lagoon

The DGD method was further applied during a field campaign in June 2017 at La Palme lagoon on the French coastline of the Mediterranean Sea. The shallow lagoon has a surface area of approximately $5\,km^2$, a mean depth of $0.6\,m$ and a maximum depth of $1.8\,m$.[1] The water level was not influenced by tides, as there was no direct hydraulic connection of the lagoon to the sea.

The small depth of the lagoon ensures the water heats up quickly in response to solar irradiation and loses heat quickly at night, which leads to large diurnal temperature variations. The lagoon is regularly exposed to strong north-westerly winds, which cause waves of a maximum amplitude of about $0.4\,m$.[1] Inflow of groundwater occurs in the northern section of the lagoon.[1] Recirculation of water between the lagoon and the pore space of shallow sediments is considerable and flows vary with up to an order of magnitude.[1,30] Such water exchange might influence the concentrations of some of the gases.[31] Particularly, He being enriched in the pore water of sediments by in-situ production or groundwater input might be subject to variations in the mixing of the water masses. Further, can O_2 be significantly consumed by the sediments. However, Ar and Kr are not affected by sediment/water exchange.[32]

The gas measurements were carried out near the center of the lagoon. Water was pumped $55\,m$ from the sampling point at a water depth of $1\,m$ to the onshore GE-MIMS system by a submersible pump through a hard plastic tube (polyamide tubing; $66\,m$ in length). Cavitation was not observed during the course of the experiments and phase separation does not result in systematic errors as long as the travelling time of both phases is the same. Mechanical filters and regular cleaning of the membrane contactors kept the flow rates high to guarantee reliable gas measurements. The travel time of the water through the hoses was estimated to be approximately $5\,min$ which is negligibly small in comparison to the diurnal variation.

Results and Discussion

Resolution and Sensitivity

The DGD method allows determination of gas exchange rates only within a certain range of k/h values. Here we discuss the upper and lower limits of the determination of the transfer velocity using the DGD approach, and elaborate on the constraining parameters.

We have run the model several times in a theoretical setting to determine the sensitivity and resolution of the method. For that purpose a synthetic sinusoidal variation in the water temperature simulate the diurnal heating and cooling. This pre-set temperature cycle has a mean temperature value of $15\,°C$, a peak-to-peak amplitude of $2\,°C$, $6\,°C$, $10\,°C$, $16\,°C$ or $20\,°C$ and a $24\,h$ period. $C_{eq,i}$ were calculated for a constant atmospheric pressure of $1013.15\,hPa$. The expected water concentrations $C_{w,i}$ are modeled for a k/h-range of $0 - 10\,d^{-1}$.

This synthetic data exercise allow us to derive upper and lower bounds for the determination of the gas transfer velocities by comparing the parameters to the experimental precision of the gas measurements. We define two quantities necessary to be resolved by the measurement setup. (D_i) is the maximum difference between the expected water concentration and the equilibrium concentration normalized to the mean equilibrium concentration of one period, $D_i = \frac{max(|C_{w,i}(t) - C_{eq,i}(t)|)}{\overline{C_{eq,i}}}$. We define (A_i) as the amplitude of the expected concentration normalized to the mean equilibrium concentration of the time series $A_i = \frac{max(C_{w,i}(t)) - min(C_{w,i}(t))}{\overline{C_{eq,i}}}$.

For very low k/h, $C_{w,i}$ approaches a constant value. The water concentrations will be approximately equal to the equilibrium concentration at the daily mean water temperature. The lower limit of resolution of k/h is shown in Fig. 1 for Ar and for the five different values of diurnal water temperature variation. In this case, the experimental setup is not sensitive to changes in k/h as the amplitude, A_{Ar} (yellow, right y-axis), due to temperature becomes less than the analytical precision (red line in Fig. 1; for Ar) of the gas measurements .

The limit is higher for lower diurnal temperature differences as the concentration gradients are smaller. For a water temperature amplitude of $10\,°C$ the lower limit is approximately $0.07\,d^{-1}$ for Ar, $0.05\,d^{-1}$ for N_2 and $0.1\,d^{-1}$ for Kr. The smaller the temperature amplitude of the daily forcing the higher the minimum of k/h that can be reliably determined.

For high k/h, the gas concentrations in surface water rapidly approaches $C_{eq,i}$, such that the difference between $C_{w,i}$ and $C_{eq,i}$ gets small. Any further increase in k/h will not produce detectable changes between the expected and the equilibrium concentration, leaving the method insensitive for large k/h. Fig. 1 shows D_{Ar} (blue, left y-axis). The upper limit of the method is the point at which the difference between the expected concentration and the equilibrium concentration becomes smaller than the analytical precision. The upper limit of the method is, therefore, reached if D_{Ar} is smaller than the analytical precision. For a diurnal temperature change of $10\,°C$, the upper limit of k/h that can be reliably measured is approximately $4\,d^{-1}$ for Ar, $9\,d^{-1}$ for N_2 and $2\,d^{-1}$ for Kr. The smaller the temperature amplitude the lower the maximum of k/h that can be reliably determined.

The range of k/h values that can be reliably determined by Ar is therefore approximately $0.07 - 4\,d^{-1}$ for a diurnal temperature variation of $10\,°C$. Results for water depths of $0.2\,m$ and $0.6\,m$ are of $0.01 - 0.8\,m/d$ and $0.04 - 2.4\,m/d$, respectively.

The ability to resolve differences in gas transfer velocity therefore depends on the magnitude of diurnal water temperature variation, on the water depth, on the temperature dependence of the solubility in water and on the measurement precision. The latter two factors are specific to each gas species.

In summary, the range of gas transfer velocities that can be determined by the DGD method falls well in the range of gas transfer velocities that are typically encountered in natural waters (average for lakes and reservoirs $1.0\,m/d$; global average $5.7\,m/d$).[33]

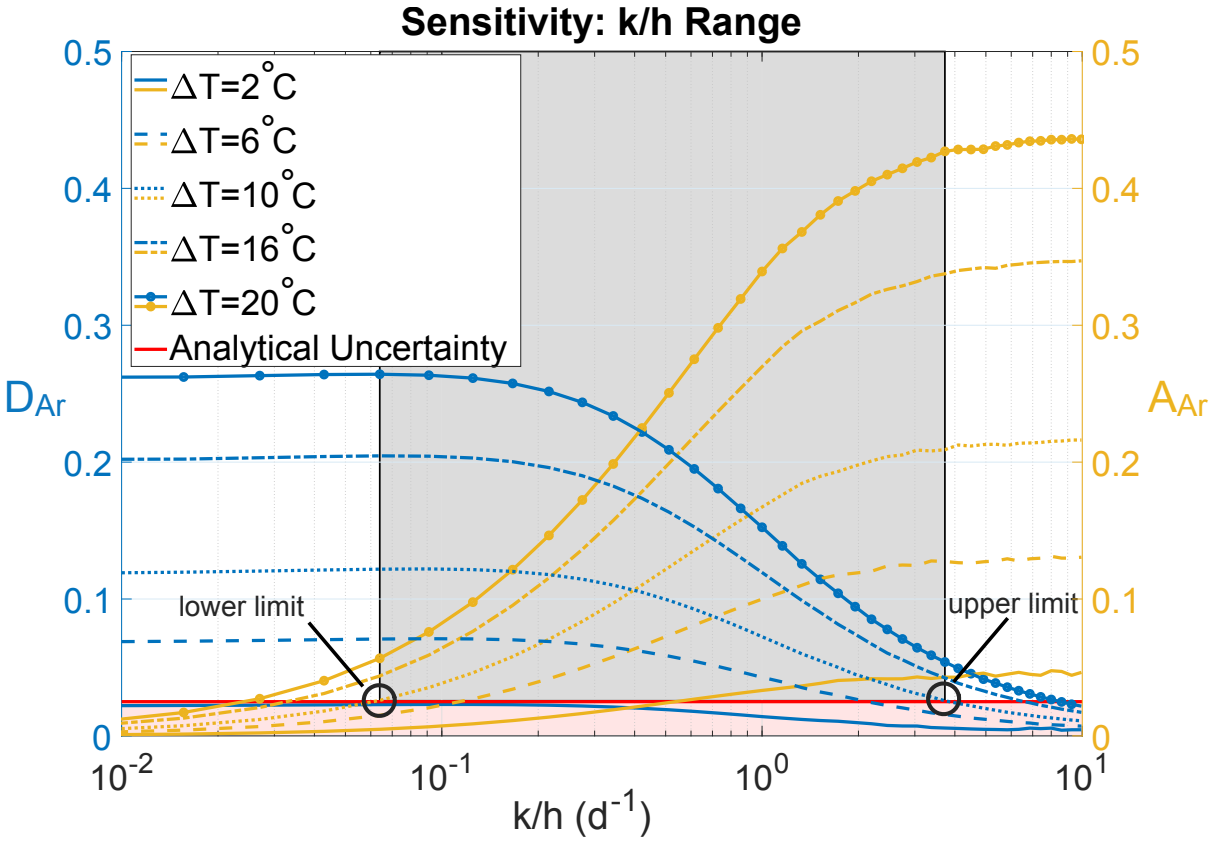

Figure 1: The maximal concentration difference between expected concentration in water and equilibrium concentration (D_{Ar}) (blue, left y-axis) and the amplitude of the water concentration (A_{Ar}) (yellow, right y-axis) both normalized to the mean equilibrium concentration shown for different water temperature amplitudes. High k/h results in a small difference between the expected and equilibrium concentrations, hence, small D_{Ar}. Where D_{Ar} is less than the experimental precision (that for Ar is indicated by the red horizontal line), $C_{eq,i}$ and $C_{w,i}$ cannot be reliably differentiated, determining the upper limit on the k/h range. At low k/h the expected diurnal concentration amplitude, A_{Ar}, is less than the experimental precision. This, therefore, defines the lower limit for k/h determination. The range for $\Delta T = 10°C$ (grey area and black circles) is approximately $0.07 - 4\,d^{-1}$ for Ar with an experimental uncertainty of 2.5 %.

Controlled Experiment

The results of the equilibrium, the observed and the modeled gas concentrations for N_2, Ar and Kr in the controlled experiment are shown in Fig. 2. The large diurnal amplitude in water temperature in the tub (up to $25\,°C$) result in large variations in $C_{eq,i}$. The observed $C_{w,i}$ are lagged and their amplitudes are damped relative to $C_{eq,i}$, as predicted by the model. Concentration changes in the dissolved gas concentrations are as high as 45 % for Kr, 16 % for Ar and 13 % for N_2 relative to the lowest measured concentration. These changes are the direct result of the different solubilities and the analytical uncertainties.

The model reproduces the measured concentrations for the gases very well. The best-fit gas exchange rates are: $k^*_{Ar} = 0.29 \pm 0.01\,m/d$, $k^*_{N_2} = 0.27 \pm 0.02\,m/d$, $k^*_{Kr} = 0.39 \pm 0.06\,m/d$. Those values result in a ratio of $k^*_{N_2}/k^*_{Ar} = 0.93 \pm 0.02$, which is, within the uncertainty, the same as the expected value of 0.95 from Eq. 5 (Schmidt numbers for fresh water at $T = 20\,°C$: $Sc_{Ar} = 552$, $Sc_{N_2} = 612$, $Sc_{Kr} = 625$[7]). For Kr the derived solution of the transfer velocity matches with that scaled from Ar with the Schmidt number ratio ($k_{SC,Kr} = 0.27\,m/d$) within its 2σ confidence interval. $k_{SC,Kr}$ also fits the data well given the scattering of the data (Fig. 2). Due to the lower experimental precision the error of the estimated gas transfer velocity is larger for Kr than for Ar and N_2.

To illustrate the ability of the DGD method to reproduce $C_{w,i}$, model results for N_2 and Ar are shown for $0.5 \cdot k^*_i$ and $1.5 \cdot k^*_i$. This exercise makes the case that the uncertainty of the estimated transfer velocities for N_2 and Ar is significantly better than ± 50 %, and mostly falls in the range between $5 - 20$ %, depending also on the length of the measured time series.

The controlled experiment demonstrates the potential of the different gases to trace gas exchange processes. Due to their low solubility and high atmospheric abundance, N_2 and Ar are particularly powerful tracers for gas exchange. The analytical noise in Kr leads to a large uncertainty in deriving the respective transfer velocity. Ar has a signal-to-noise ratio that is only slightly higher than that of N_2. These differences between gases are fully explained by the abundance and the analytical performance of the applied GE-MIMS method to determine

gas concentrations.[16]

In summary, we interpret the controlled experiment as a proof of concept of the DGD method.

Field Study at La Palme Lagoon

Fig. 3 shows the results of the equilibrium, the observed and the modeled gas concentrations of the La Palme lagoon. The diurnal temperature variation was up to $10\,°C$, significantly less than in the tub experiment. For such smaller diurnal temperature amplitudes the experimental errors of the Kr measurements are too large to estimate the gas transfer velocity in a robust manner. Therefore, in the following only N_2 and Ar results are shown and discussed.

The model reproduces the observed data for N_2 remarkably well. Ar concentrations are also reproduced correctly for a large period of the time series. However, in the morning of the second day we observed a decrease in Ar concentrations which are not captured by our simple model. The low concentration may relate to a specific (but unidentified) event or process which affect the Ar but not the N_2 concentration. Such deviation between the measured and the modeled concentration shows how valuable time series of gas measurements over several days are, as they inform on additional processes that affect atmospheric gases in aquatic systems besides atmospheric exchange. However, we have no appropriate explanation for the observed deviation between the measured and predicted Ar concentration.

For N_2 two periods with different response dynamics of the in-situ concentrations to the diurnal heating can be observed (indicated with different colors in Fig. 3). For the first period which lasts approximately for the first two and a half days the observed N_2 concentrations are highly damped relative to the atmospheric equilibrium concentrations. For the second period the dampening of the measured to the equilibrium concentrations is much smaller. Further, the phase lag decreases from the first to the second period. Consequently, for the two periods very differing transfer velocities prevail. For the first period: $k^*_{N_2} = 1.6 \pm 0.2\,m/d$. For the second period: $k^*_{N_2} = 7.1 \pm 0.6\,m/d$. Leaving the described discrepancy on the second

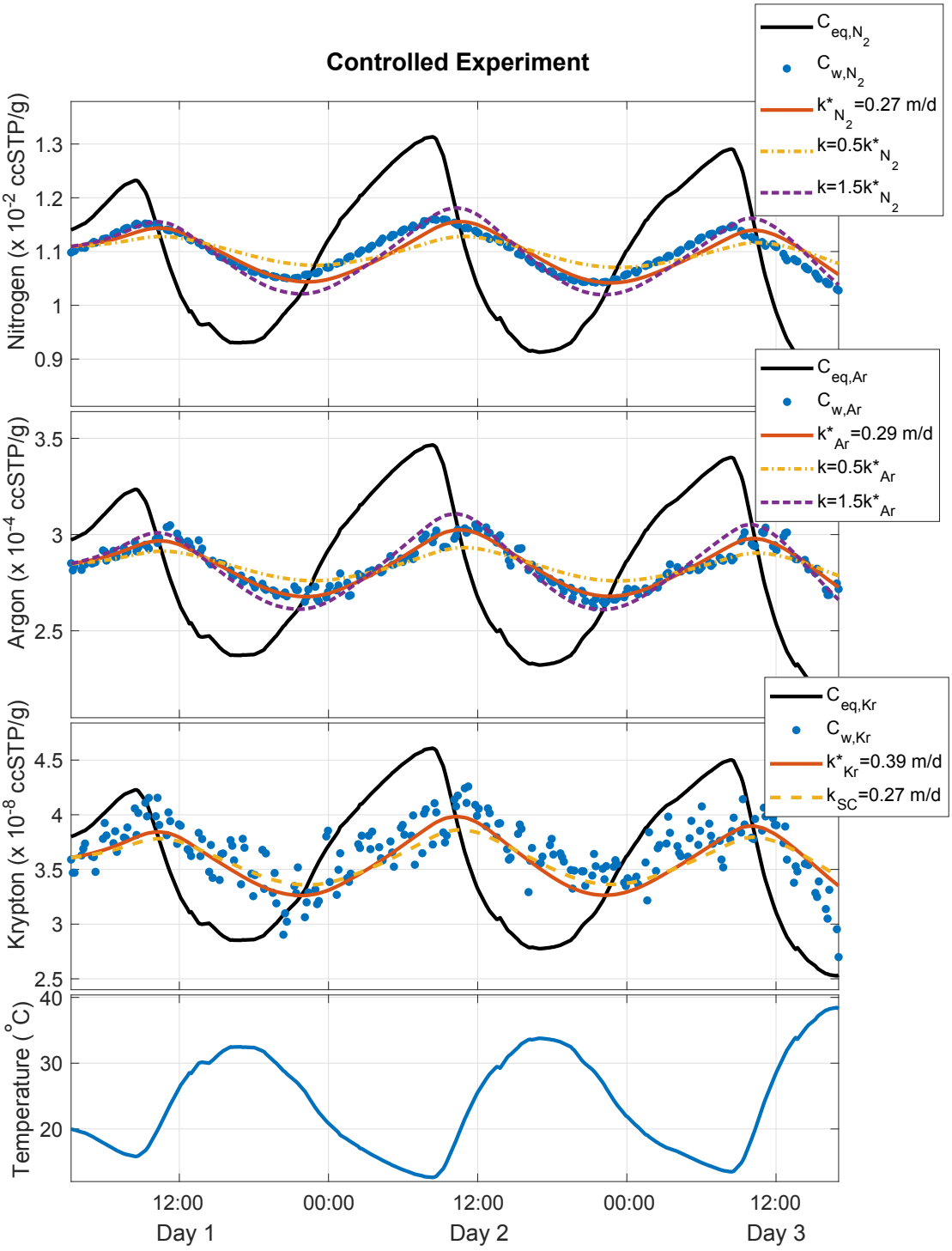

Figure 2: The equilibrium, the observed and the modeled concentrations for N_2, Ar and Kr (in $ccSTP/g$) and the water temperature for the controlled experiment and the respective transfer velocities (k_i). The model fits the gas concentrations well. The derived gas exchange rates k^* are: $k^*_{N_2} = 0.27\,m/d$, $k^*_{Ar} = 0.29\,m/d$, $k*_{Kr} = 0.39\,m/d$. To illustrate the sensitivity of the DGD method, transfer velocities 50 % larger and smaller than k^*_i are shown for N_2 and Ar. For Kr the result expected of the transfer velocity scaled from Ar with the Schmidt numbers is additionally shown (k_{SC} for Kr).

day out for Ar, globally, the same behavior can be found in the Ar time series.

The measurement position within the lagoon is rather sheltered against wind (fetch of approximately $50\,m$). Thus, during wind-calm conditions waves rapidly dissipate. During the first period wind speeds were low (mean wind speed $\overline{u}_{10} = 2.9\,m/s$; u_{10}: measured wind speed scaled to ten meters above the water surface[34]), while during the second period wind speeds more than three times higher were observed ($\overline{u}_{10} = 10.2\,m/s$). This change was also found in the transfer velocity, and demonstrates the ability of the method to resolve different weather conditions on time scales of hours to days.

Discussion

The controlled and the La Palme lagoon experiments demonstrate the capability of the DGD method to quantify temporally changing gas exchange rates at specific locations and on relative short time scales. The presented method allows the quantification of the transfer velocity over the wide range of approximately $0.05{-}9\,m/d$ (for N_2), which covers the typically observed range of gas transfer for surface waters. The quantifiable range in k/h depends on the magnitude of the diurnal water temperature variation, the temperature dependence of the gas solubility in water and on the measurement precision.

The selection of gases being used as tracers by our method depends on the environmental processes the respective gases are undergoing and on the experimental setup. The noble gases He, Ne, Ar, Kr, Xe and Rn are best suited due to their inert behavior, whereas the gases O_2 and N_2 are subject to biochemical reactions. However, the noble gases He and Rn, in contrast to Ar, Kr and Xe, are released from the sediments by radioactive decay and their concentrations, therefore, depend on e.g. groundwater inflow and circulation of water between surface water and sediments.

From a technical perspective of the noble gases, currently only He, Ar and Kr can be analyzed quasi-continuously, whereas in-situ measurement capability for Ne and Xe using our GE-MIMS instrument remains to be developed. On-going improvements of the experimental

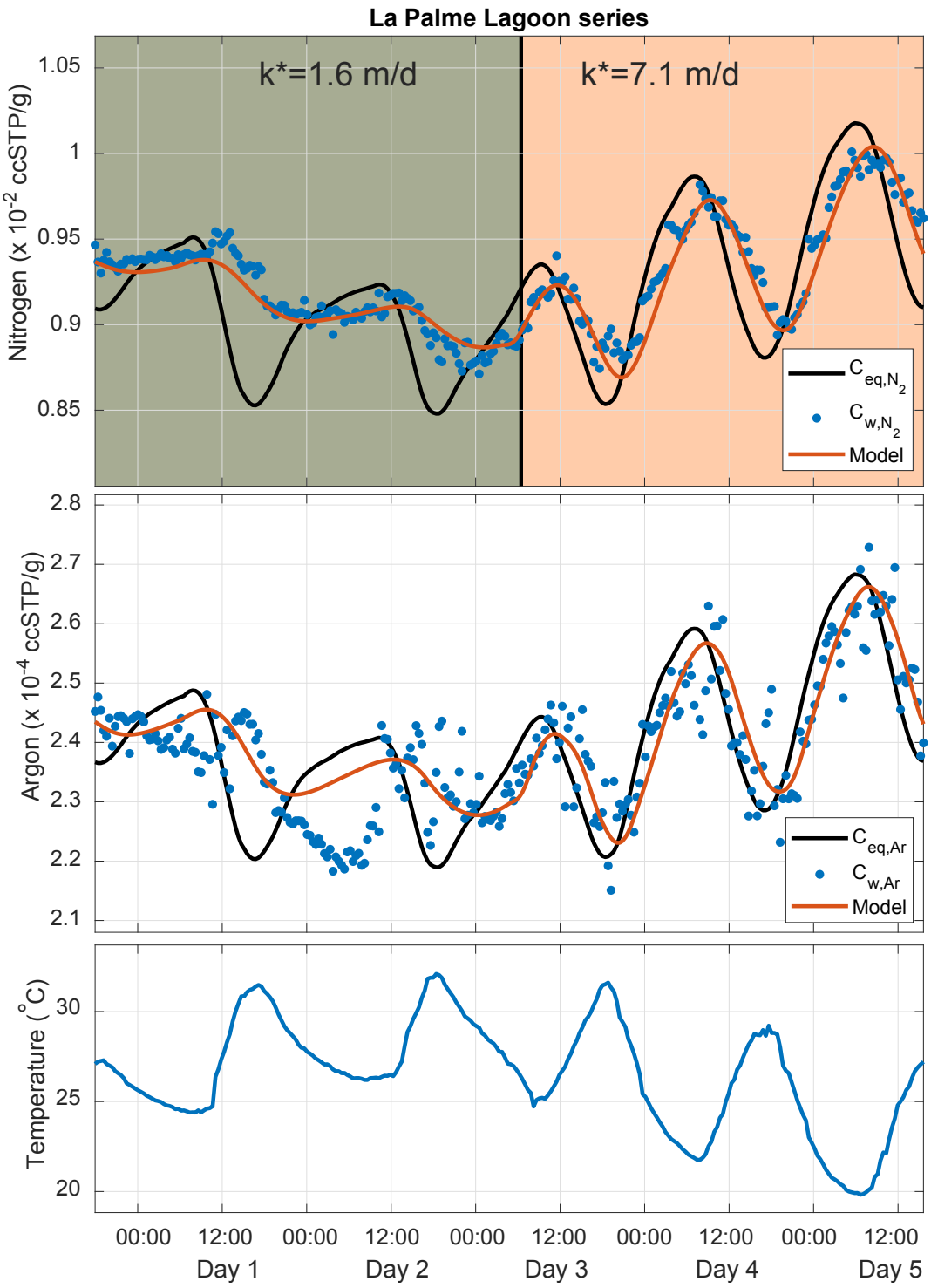

Figure 3: The equilibrium, the observed and the modeled concentrations for N_2 and Ar (in $ccSTP/g$) and the water temperature series of the water in La Palme Lagoon. The derivation of the transfer velocity for N_2 with the DGD method is split into two periods. The first 2.5 days (green) result in a transfer velocity of $k^*_{N_2} = 1.6 \pm 0.2\, m/d$, while the second 2.5 days (orange) result in $k^*_{N_2} = 7.1 \pm 0.6\, m/d$. Those phases are characterized by very different wind regimes with $\overline{u}_{10} = 2.9\, m/s$ for the first and $\overline{u}_{10} = 10.2\, m/s$ for the second phase.

performance of (GE)-MIMS systems might increase the number of gases that can be used to analyze air/water partitioning and, thus, greatly expand the determinable range (and the accuracy) of k/h values.

Our experiments show that N_2 and Ar are most sensitive to gas transfer velocities under field conditions given the available technology. N_2 yields the widest k/h range as it has the best signal-to-noise ratio. However, N_2 is potentially non-conservative due to biogeochemical processes, such as denitrification.

The DGD method works best for large daily temperature changes in the water; preferably a water temperature variation of $10\,^{\circ}C$ prevails to get reliable results and to cover a relevant range of gas transfer velocities. Such high variations are more likely to be found in shallow waters with depths less than a few meters, furthermore, deeper water is unlikely to be vertically well mixed as assumed in our model. Additionally, local conditions can influence the diurnal temperature cycles, including solar radiation, water residence time and heat absorption. These impact the applicability of this method. In rivers, for example, where the method is applicable in principle,[15] this temperature requirement is currently the limiting factor and could be rare to find. Again, improvements in gas measurements expand the locations that can be covered.

The DGD method can be used to quantify temporal variations in transfer velocities, which can then be linked to environmental drivers of air-water exchange, such as wind or river-flow-driven turbulence. For instance, measuring k_i over a few days with varying wind speeds could be used to derive relationships between transfer velocity and wind speed in shallow environments. It may also be possible to determine the influence of parameters (e.g. precipitation) on near surface turbulence that are less frequently incorporated into the estimation of the gas transfer velocity.

The mass spectrometer used in this study can cycle through multiple inlets on a time scales of minutes, which allows automated analysis at several locations simultaneously. This allows coverage of different geographic conditions at sites, that may be more complex than

the open ocean. Hence, site-specific parametrizations can be derived on several orders of areal extents.

As the DGD method does not rely on the application of any artificial tracer, there is no contamination of the environment. With additionally determined quantities e.g. tidal influences, groundwater intrusion or deep water mixing a more complete description of a study site is possible.

Alternative approaches for measuring air-water gas exchange are more labor intensive and have limited temporal resolution. The DGD method presented here, thus has the potential to greatly improve on the ability to measure air-water exchange in shallow waters.

Acknowledgements

We gratefully thank Aladin Andrisoa, Anne Brennwald, Marine David, Alexandra Lightfoot and Valenti Rodellas for conducting the field measurements with us. Furthermore, we thank three anonymous reviewers for their constructive comments.

This research is a contribution to the ANR @RAction chair medLOC (ANR-14-ACHN-0007-01, T. Stieglitz) and Labex OT-Med (ANR-11-LABEX-0061, part of the "Investissements d'Avenir" program through the A/MIDEX project ANR-11-IDEX-0001-02), funded by the French National Research Agency (ANR). PC acknowledges support from IMéRA (Institute of Advanced Studies), Aix-Marseille Université (Labex RFIEA and ANR "Investissements d'avenir").

References

(1) Stieglitz, T. C.; van Beek, P.; Souhaut, M.; Cook, P. G. Karstic groundwater discharge and seawater recirculation through sediments in shallow coastal Mediterranean lagoons, determined from water, salt and radon budgets. *Marine Chemistry* **2013**, *156*, 73–84.

(2) Cook, P. G.; Lamontagne, S.; Berhane, D.; Clark, J. F. Quantifying groundwater discharge to Cockburn River, southeastern Australia, using dissolved gas tracers 222 Rn and SF6. *Water Resources Research* **2006**, *42*, W10411.

(3) Gleeson, T.; Manning, A. H.; Popp, A.; Zane, M.; Clark, J. F. The suitability of using dissolved gases to determine groundwater discharge to high gradient streams. *Journal of Hydrology* **2018**, *557*, 561–572.

(4) Cole, J. J.; Prairie, Y. T.; Caraco, N. F.; McDowell, W. H.; Tranvik, L. J.; Striegl, R. G.; Duarte, C. M.; Kortelainen, P.; Downing, J. A.; Middelburg, J. J.; Melack, J. Plumbing the Global Carbon Cycle: Integrating Inland Waters into the Terrestrial Carbon Budget. *Ecosystems* **2007**, *10*, 172–185.

(5) Heinze, C.; Meyer, S.; Goris, N.; Anderson, L.; Steinfeldt, R.; Chang, N.; Quéré, C. L.; Bakker, D. C. E. The ocean carbon sink – impacts, vulnerabilities and challenges. *Earth System Dynamics* **2015**, *6*, 327–358.

(6) Qiu, X.; Zhu, T.; Wang, F.; Hu, J. Air–Water Gas Exchange of Organochlorine Pesticides in Taihu Lake, China. *Environmental Science & Technology* **2008**, *42*, 1928–1932.

(7) Wanninkhof, R. Relationship between wind speed and gas exchange over the ocean revisited. *Limnology and Oceanography: Methods* **2014**, *12*, 351–362.

(8) Khadka, M. B.; Martin, J. B.; Kurz, M. J. Synoptic estimates of diffuse groundwater seepage to a spring-fed karst river at high spatial resolution using an automated radon measurement technique. *Journal of Hydrology* **2017**, *544*, 86–96.

(9) Ashton, I. G.; Shutler, J. D.; Land, P. E.; Woolf, D. K.; Quartly, G. D. A Sensitivity Analysis of the Impact of Rain on Regional and Global Sea-Air Fluxes of CO2. *PLOS ONE* **2016**, *11*, e0161105.

(10) Ho, D. T.; Bliven, L. F.; Wanninkhof, R.; Schlosser, P. The effect of rain on air-water gas exchange. *Tellus B* **1997**, *49*, 149–158.

(11) Ho, D. T.; Coffineau, N.; Hickman, B.; Chow, N.; Koffman, T.; Schlosser, P. Influence of current velocity and wind speed on air-water gas exchange in a mangrove estuary. *Geophysical Research Letters* **2016**, *43*, 3813–3821.

(12) Watson, A. J.; Upstill-Goddard, R. C.; Liss, P. S. Air–sea gas exchange in rough and stormy seas measured by a dual-tracer technique. *Nature* **1991**, *349*, 145–147.

(13) Hall Jr., R. O.; Madinger, H. L. Use of argon to measure gas exchange in turbulent mountain streams. *Biogeosciences* **2018**, *15*, 3085–3092.

(14) Knapp, J. L.; Osenbrück, K.; Brennwald, M. S.; Cirpka, O. A. In-situ mass spectrometry improves the estimation of stream reaeration from gas-tracer tests. *Science of The Total Environment* **2019**, *655*, 1062–1070.

(15) Sanford, W. E.; Casile, G.; Haase, K. B. Dating base flow in streams using dissolved gases and diurnal temperature changes. *Water Resources Research* **2015**, *51*, 9790–9803.

(16) Brennwald, M. S.; Schmidt, M.; Oser, J.; Kipfer, R. A Portable and Autonomous Mass Spectrometric System for On-Site Environmental Gas Analysis. *Environmental Science & Technology* **2016**, *50*, 13455–13463.

(17) Manning, C. C.; Stanley, R. H. R.; Lott, D. E. Continuous Measurements of Dissolved Ne, Ar, Kr, and Xe Ratios with a Field-Deployable Gas Equilibration Mass Spectrometer. *Analytical Chemistry* **2016**, *88*, 3040–3048.

(18) Chatton, E.; Labasque, T.; de La Bernardie, J.; Guihéneuf, N.; Bour, O.; Aquilina, L. Field Continuous Measurement of Dissolved Gases with a CF-MIMS: Applications to the Physics and Biogeochemistry of Groundwater Flow. *Environmental Science & Technology* **2016**, *51*, 846–854.

(19) Schwarzenbach, R. P.; Gschwend, P. M.; Imboden, D. M. *Environmental Organic Chemistry*; John Wiley & Sons, Inc., 2016.

(20) Kipfer, R.; Aeschbach-Hertig, W.; Peeters, F.; Stute, M. Noble Gases in Lakes and Ground Waters. *Reviews in Mineralogy and Geochemistry* **2002**, *47*, 615–700.

(21) Weiss, R. The solubility of nitrogen, oxygen and argon in water and seawater. *Deep Sea Research and Oceanographic Abstracts* **1970**, *17*, 721–735.

(22) Weiss, R. F.; Kyser, T. K. Solubility of krypton in water and sea water. *Journal of Chemical & Engineering Data* **1978**, *23*, 69–72.

(23) Sander, R. Compilation of Henry's law constants for inorganic and organic species of potential importance in environmental chemistry. 1999.

(24) Jähne, B.; Münnich, K. O.; Bösinger, R.; Dutzi, A.; Huber, W.; Libner, P. On the parameters influencing air-water gas exchange. *Journal of Geophysical Research* **1987**, *92*, 1937.

(25) Etcheto, J.; Merlivat, L. Satellite determination of the carbon dioxide exchange coefficient at the ocean-atmosphere interface: A first step. *Journal of Geophysical Research* **1988**, *93*, 15669–15678.

(26) Press, W. H.; Teukolsky, S. A.; Vetterling, W. T.; Flannery, B. P. *Numerical recipes 3rd edition: The art of scientific computing*; Cambridge university press, 2007.

(27) Savitzky, A.; Golay, M. J. Smoothing and differentiation of data by simplified least squares procedures. *Analytical chemistry* **1964**, *36*, 1627–1639.

(28) Mächler, L.; Brennwald, M. S.; Kipfer, R. Membrane Inlet Mass Spectrometer for the Quasi-Continuous On-Site Analysis of Dissolved Gases in Groundwater. *Environmental Science & Technology* **2012**, *46*, 8288–8296.

(29) Mächler, L.; Brennwald, M. S.; Tyroller, L.; Livingstone, D. M.; Kipfer, R. Conquering the Outdoors with On-site Mass Spectrometry. *CHIMIA International Journal for Chemistry* **2014**, *68*, 155–159.

(30) Rodellas, V.; Stieglitz, T. C.; Andrisoa, A.; Cook, P. G.; Raimbault, P.; Tamborski, J. J.; van Beek, P.; Radakovitch, O. Groundwater-driven nutrient inputs to coastal lagoons: The relevance of lagoon water recirculation as a conveyor of dissolved nutrients. *Science of The Total Environment* **2018**, *642*, 764–780.

(31) Cook, P. G.; Rodellas, V.; Stieglitz, T. C. Quantifying Surface Water, Porewater, and Groundwater Interactions Using Tracers: Tracer Fluxes, Water Fluxes, and End-member Concentrations. *Water Resources Research* **2018**, *54*, 2452–2465.

(32) Brennwald, M. S.; Vogel, N.; Scheidegger, Y.; Tomonaga, Y.; Livingstone, D. M.; Kipfer, R. *The Noble Gases as Geochemical Tracers*; Springer Berlin Heidelberg, 2013; pp 123–153.

(33) Raymond, P. A.; Hartmann, J.; Lauerwald, R.; Sobek, S.; McDonald, C.; Hoover, M.; Butman, D.; Striegl, R.; Mayorga, E.; Humborg, C.; Kortelainen, P.; Dürr, H.; Meybeck, M.; Ciais, P.; Guth, P. Global carbon dioxide emissions from inland waters. *Nature* **2013**, *503*, 355–359.

(34) Foken, T. *Micrometeorology*; Springer Berlin Heidelberg, 2017.